Synthesis of Triruthenium–Rhodium Tetranuclear Clusters derived from $[Ru_3H_3(CO)_9(\mu_3\text{-COMe})]$. Crystal Structure of $[N(PPh_3)_2][Ru_3RhH_2(CO)_{11}(PPh_3)]\cdot 0.6C_5H_{12}$†

John Evans,* Philip M. Stroud and Michael Webster
Department of Chemistry, University of Southampton, Southampton SO9 5NH, UK

Reaction of $K[Ru_3H_2(CO)_9(\mu_3\text{-COMe})]$ with $[Rh(CO)_3(PPh_3)_2][PF_6]$ affords $[Ru_3H_2(CO)_9(\mu_3\text{-COMe})\{Rh(CO)_2(PPh_3)\}]$ **3** in 80% yield, with $[Ru_3H(CO)_9(PPh_3)(\mu\text{-COMe})]$, $[Ru_3H(CO)_8(PPh_3)_2(\mu\text{-COMe})]$ and $[Ru_3RhH_2(CO)_8(PPh_3)_3(\mu\text{-COMe})]$ as minor products; $[Ru_3RhH_2(CO)_9(PPh_3)_2(\mu\text{-COMe})]$ **8** was isolated from the corresponding reaction with $[Rh(CO)(PPh_3)_2Cl]$ and exists as five interconverting isomers in solution. At room temperature **3** loses one CO group to form the tetrahedral cluster $[Ru_3RhH_2(CO)_{10}(PPh_3)(\mu\text{-COMe})]$ **7**. This consists of two isomers in solution, with the major one being the molecular structure observed in the crystal. On reaction with $K[BHBu^s_3]$, complex **7** undergoes a demethylation reaction to form $[N(PPh_3)_2][Ru_3RhH_2(CO)_{11}(PPh_3)]$ **9**. A single-crystal X-ray diffraction study of $[N(PPh_3)_2][Ru_3RhH_2(CO)_{11}(PPh_3)]\cdot 0.6C_5H_{12}$ was carried out: triclinic, space group $P1$ (no. 1), $a = 12.244(2)$, $b = 13.453(3)$, $c = 11.926(3)$ Å, $\alpha = 111.40(2)$, $\beta = 101.30(2)$, $\gamma = 70.02(1)°$, $Z = 1$, $R = 0.053$ from 4349 observations $[F > 3\sigma(F)]$. This showed a structure derived from $[Rh_4(CO)_{12}]$, with an apical $Ru(CO)_2(PPh_3)$ unit, and the Rh atom in the basal plane. The two hydrides were not located directly, but are considered to bridge apical–basal Ru–Ru edges.

It has previously been shown that the methoxymethylidyne ligand can maintain its face-bridging site on a triruthenium cluster as a fourth, coinage-metal, atom is added.[1,2] We were concerned to extend the synthesis of heterometallic clusters to include ruthenium–rhodium species, in view of the reported synergistic effects of these two metals in some catalytic systems.[3–5] Considerable interest has been shown in the synthesis of such clusters.[6–9] However in view of our experience of the ready fragmentation of clusters in the course of reactions,[10,11] we directed our synthesis towards ligand-stabilised clusters, concentrating on a carbyne ligand, rather than alternatives such as multidentate phosphines,[12] interstitial atoms[13] or phosphinidene ligands.[14] A brief report of some of this work has been presented.[15]

Experimental

The general experimental procedures were as described in ref. 1, with the additional facility of fast atom bombardment (FAB) mass spectra on a VG 70-250SE instrument using *m*-nitrobenzyl alcohol as the matrix. The following compounds were prepared by established methods: $[Rh(CO)_3(PPh_3)_2][PF_6]$,[16] $[Ru_3H(CO)_{10}(\mu\text{-COMe})]$,[17] $[Ru_3H_3(CO)_9(\mu_3\text{-COMe})]$ **1**,[18] $K[Ru_3H_2(CO)_9(\mu_3\text{-COMe})]$ **2**,[1] and $[Rh(CO)(PPh_3)_2Cl]$.[19]

Preparations.—$[Ru_3H_2(CO)_9(\mu_3\text{-COMe})\{Rh(CO)_2(PPh_3)\}]$ **3**. To a solution of $K[Ru_3H_2(CO)_9(\mu_3\text{-COMe})]$ **2** (from 2.00 g **1**, 3.33 mmol) in MeOH (150 cm^3) at −20 °C was added solid $[Rh(CO)_3(PPh_3)_2][PF_6]$ (3.00 g, 3.50 mmol). The required product immediately began to precipitate along with a white solid. After 5 min the mixture was allowed to warm to room temperature and stirred for 40 min. After this period the white precipitate had dissolved and compound **3** was collected by filtration as an orange-red solid which was thoroughly washed with MeOH (8 × 20 cm^3) to ensure complete removal of KPF_6, yield 2.71 g (80%) (Found: C, 36.6; H, 2.0. $C_{31}H_{20}O_{12}PRhRu_3$ requires C, 36.5; H, 2.0%). FAB mass spectrum included M^+ at m/z = 1023. Compound **3** is very soluble in CH_2Cl_2 and tetrahydrofuran (thf), partially soluble in non-polar organic solvents, and practically insoluble in MeOH. IR: ν(CO) (cyclohexane) 2095m, 2070m, 2043vs, 2034vs, 2004s, 1981vw, 1972w, 1957w and 1930vw cm^{-1}. NMR: ^{1}H (CD_2Cl_2, 273 K), δ 7.7–7.1 (m, Ph, 15 H), 4.06 (s, OMe, 3 H) and −18.02 (dd, J_1 = 1.5, J_2 = 1, μ-H, 2 H); ^{31}P-{^{1}H} ($CDCl_3$, 253 K), δ 32.2 [d, *J*(RhP) 139]; ^{13}C-{^{1}H} (CD_2Cl_2, 263 K), δ 287.1 (s, *C*OMe), 209.2 (s, 2 C), 205.7 [dd, *J*(RhC) 56, *J*(PC) 13, 1 C], 203.6 [dd, *J*(RhC) 61, *J*(PC) 13 Hz, 1 C], 197.1 (s, 2 C), 192.6 (s, 3 C), 189.0 (s, 2 C), 136–127 (Ph) and 69.6 (s, CO*Me*).

$[Ru_3H(CO)_9(PPh_3)(\mu\text{-COMe})]$ **4**, $[Ru_3H(CO)_8(PPh_3)_2(\mu\text{-COMe})]$ **5** *and* $[Ru_3RhH_2(CO)_8(PPh_3)_3(\mu\text{-COMe})]$ **6**. The filtrate from the preceding preparation was evaporated to dryness and the solid residue chromatographed on a silica column. Compounds **4** and **5** were isolated as yellow and red-orange solids from the second and third bands respectively using light petroleum (b.p. 40–60 °C)–CH_2Cl_2 (4:1 v/v) as the eluent for **4** (154 mg, 5%) and a similar 2:1 mixture for **5** (58 mg, 1.5%). A fourth deep red band was collected using a 1:1 v/v eluent mixture. The red solid isolated from this band was dissolved in the minimum quantity of CH_2Cl_2 (*ca.* 1 cm^3) and compound **6** precipitated from this solution by addition of EtOH (15 cm^3). Collection by filtration and washing with EtOH (3 × 10 cm^3) gave **6** (101 mg, 2%) as a pale orange solid. Compounds **4** and **5** can be recrystallised from CH_2Cl_2 and hexane with cooling; they are very soluble in CH_2Cl_2 and partially soluble in non-polar organic solvents and MeOH. Compound **6** is soluble in CH_2Cl_2, practically insoluble in non-polar organic solvents, and insoluble in MeOH.

Compound **4** (Found: C, 40.4; H, 2.1. $C_{29}H_{19}O_{10}PRu_3$ requires C, 40.4; H, 2.2%). IR: ν(CO) (cyclohexane) 2085s, 2046vs, 2014vs, 2005s, 1992s, 1989(sh), 1980m, 1975m, 1971m and 1956w cm^{-1}. NMR ($CDCl_3$): ^{1}H, δ 7.5–7.3 (m, Ph, 15 H), 4.08 (s, OMe, 3 H) and −14.17 [d, *J*(PH) 8, μ-H, 1 H]; ^{31}P-{^{1}H},

---

† Bis(triphenylphosphoranylidene)ammonium tri-μ-carbonyl-1:3κ^2*C*; 1:4κ^2*C*; 3:4κ^2*C*-octacarbonyl-1κ^2*C*,2κ^2*C*,3κ^2*C*,4κ^2*C*-di-μ-hydrido-1:2κ^2*H*; 2:3κ^2*H*-triphenylphosphine-2κ*P*-*tetrahedro*-rhodiumtriruthenate–pentane (1/0.6).

Supplementary data available: see Instructions for Authors, *J. Chem. Soc., Dalton Trans.*, 1991, Issue 1, pp. xviii–xxii.

δ 40.4 (s); ^{13}C-{^1H}, δ 372.7 (s, *C*OMe), 206.4 [d, *J*(PC) 9 Hz, 1 C], 204.2 (br, 2 C), 200.4 (s, 2 C), 197.2 (s, 1 C), 196.1 (br, 2 C), 188.7 (s, 1 C), 138–127 (Ph) and 73.7 (s, CO*Me*).

Compound **5** (Found: C, 50.2; H, 3.2. $C_{46}H_{34}O_9P_2Ru_3$ requires C, 50.4; H, 3.1%). IR: ν(CO) (cyclohexane) 2062m, 2021vs, 1999vs, 1994(sh), 1972s and 1963s cm^{-1}. NMR ($CDCl_3$): ^1H, δ 7.6–7.2 (m, Ph, 30 H), 3.91 (s, OMe, 3 H) and −13.85 [dd, *J*(P^1H) 7, *J*(P^2H) 2, μ-H, 1 H]; ^{31}P-{^1H}, δ 38.7 [d, *J*(PP) 7] and 38.2 [d, *J*(PP) 7]; ^{13}C-{^1H}, δ 366.5 (s, *C*OMe), 208 (br), 207.9 [d, *J*(PC) 8 Hz], 202.7 (s), 200.4 (s), 189.0 (s), 138–127 (Ph) and 72.9 (s, CO*Me*).

Compound **6** (Found: C, 52.7; H, 3.4. $C_{64}H_{50}O_9P_3RhRu_3$ requires C, 52.6; H, 3.5%). IR: ν(CO) (CH_2Cl_2) 2022vs, 2003vs, 1978s, 1947s, 1926m and 1852w cm^{-1}. NMR ($CDCl_3$): ^1H, δ 7.5–6.8 (m, Ph, 45 H), 4.44 (s, OMe, 3 H), −15.79 [dtt, *J*(RhH) 19.5, *J*(PH) 9, *J* 2, μ-H, 1 H] and −17.27 (m, μ-H, 1 H); ^{31}P-{^1H}, δ 35.3 (m), 37.4 [ddd, *J*(RhP) 149, *J*(PP) 43, *J*(PP) 2] and 45.0 [dd, *J*(PP) 43, *J*(RhP) 5]; ^{13}C-{^1H}, δ 391.1 (s, *C*OMe), 230.1 [d, *J*(PC) 12, 1 C], 218.6 (s, 1 C), 200.8 (s, 1 C), 200.3 (s, 1 C), 199.6 (s, 1 C), 192.4 (s and d overlapping, 2 C), 188.9 [d, *J*(RhC) 72 Hz, 1 C], 138–128 (Ph) and 72.9 (s, CO*Me*).

[$Ru_3RhH_2(CO)_{10}(PPh_3)$(μ-COMe)] **7**. A solution of compound **3** (1.00 g, 0.979 mmol) in thf (150 cm^3) was stirred at room temperature until the bands due to **3** had disappeared from the IR spectrum (*ca.* 80 min). The resulting solution was evaporated to dryness and the solid residue chromatographed on a silica column. The required product was isolated as a red oil from the third band (red) with light petroleum–CH_2Cl_2 (3:1 v/v) as eluent. Scratching the red oil led to rapid solidification and gave compound **7** as a red-brown solid (486 mg, 50%). Compound **7** was purified by recrystallisation from CH_2Cl_2 and pentane with cooling [washing with pentane at −20 °C (3 × 10 cm^3)] (Found: C, 36.0; H, 2.0. $C_{30}H_{20}O_{11}PRhRu_3$ requires C, 36.3; H, 2.0%). The FAB mass spectrum shows M^+ (*m/z* 995) and loss of *n*CO (*n* = 1–10). The compound is very soluble in CH_2Cl_2 and thf and moderately soluble in non-polar organic solvents. IR: ν(CO) (cyclohexane) 2091w, 2083(sh), 2075s, 2054m, 2040vs, 2030vs, 2013vs, 1994m, 1982m, 1973m, 1963m, 1949w and 1877w cm^{-1}. NMR: ^1H (CD_2Cl_2), δ 7.7–7.3 (m, Ph, 15 H), 4.71, 4.61 (2s, COMe, total 3 H), −17.65 [t, *J*(RhH) 9.5, *J*(PH) 9.5] and −18.28 [dd, *J*(RhH) 8.5, *J*(PH) 5, μ-H, hydride, total 2 H]; ^{31}P-{^1H} ($CDCl_3$), δ 37.6 [d, *J*(RhP) 140] and 41.2 [d, *J*(RhP) 2 Hz].

[$Ru_3RhH_2(CO)_9(PPh_3)_2$(μ-COMe)] **8**. To a solution of K[$Ru_3H_2(CO)_9$(μ_3-COMe)] **2** (from 270 mg **1**, 0.450 mmol) in thf (50 cm^3) at room temperature was added solid [Rh(CO)$(PPh_3)_2$Cl] (315 mg, 0.456 mmol) and the resultant solution stirred for 60 min. After evaporation to dryness the solid residue was chromatographed on a silica column and the required product isolated as a red solid from the fourth band (orange-red) using light petroleum–CH_2Cl_2 (2:1 v/v) as the eluent. As efficient recrystallisation proved difficult due to the solubility of compound **8**, further purification by a second chromatographic separation (*via* column chromatography or preparative TLC) was used to ensure adequate purity, yield 110 mg (20%) (Found: C, 45.8; H, 3.0. $C_{47}H_{35}O_{10}P_2RhRu_3$ requires C, 46.0; H, 2.9%). The FAB mass spectrum showed M^+ (*m/z* 1229). Compound **8** is very soluble in CH_2Cl_2 and thf and moderately soluble in non-polar organic solvents and MeOH. IR: ν(CO) (cyclohexane) 2056s, 2022vs, 2006vs, 1993s, 1986m, 1972(sh), 1962s, 1951m, 1942(sh), 1898w and 1868vw cm^{-1}. ^1H NMR (89.55 MHz, CD_2Cl_2): δ 7.8–6.8 (m, Ph, 30 H), 4.76, 4.34, 4.29, 4.11 (4s, COMe, total 3 H), −15.9 and −18.4 (vbr, μ-H, total 2 H).

[$N(PPh_3)_2$][$Ru_3RhH_2(CO)_{11}(PPh_3)$] **9**. A thf solution (20 cm^3) of compound **7** (142 mg, 0.143 mmol) at room temperature was treated with 1.0 mol dm^{-3} K[$BHBu^s_3$]–thf solution (0.143 mmol). This mixture was then stirred for 15 min and [$N(PPh_3)_2$]Cl (114 mg, 0.20 mmol) and CH_2Cl_2 (15 cm^3) added. After stirring for 15 min the resultant solution was evaporated to dryness and the solid residue chromatographed on a silica column. The required product was isolated as an orange-yellow solid (72 mg, 33%) from the second band (bright orange) using CH_2Cl_2–light petroleum (2:1 v/v) as the eluent. Compound **9** was purified by recrystallisation from EtOH and pentane [washing with pentane (3 × 10 cm^3)] (Found: C, 53.0; H, 3.2. $C_{65}H_{47}NO_{11}P_3RhRu_3\cdot 0.6C_5H_{12}$ requires C, 52.3; H, 3.5%). It is very soluble in CH_2Cl_2, moderately soluble in EtOH, and insoluble in non-polar organic solvents. IR: ν(CO) (CH_2Cl_2) 2043s, 2008vs, 1989vs, 1950s, 1944(sh), 1930(sh), 1850w, 1817m and 1785s cm^{-1}. NMR: ^1H ($CDCl_3$) δ 7.7–7.1 (m, Ph, 45 H) and −19.42 [d, *J*(PH) 10, μ-H, 2 H]; ^{31}P-{^1H} ($CDCl_3$), δ 21.0 (s) and 42.5 [d, *J*(RhP) 2]; ^{13}C-{^1H} (CD_2Cl_2, 183 K), δ 266.7 (s, 1 C), 255.5 [d, *J*(PC) 22, 2 C], 201.0 (s, 2 C), 200.2 (s, 2 C), 193.8 (s, 2 C), 192.5 [d, *J*(RhC) 74, 1 C], 183.0 [dd, *J*(RhC) 64, *J*(PC) 18 Hz, 1C] and 136–125 (Ph).

X-Ray Crystal Structure Determination of [$N(PPh_3)_2$][$Ru_3RhH_2(CO)_{11}(PPh_3)$]$\cdot 0.6C_5H_{12}$.—Suitable crystals of the pentane solvate of compound **9** were grown as yellow rectangular blocks by slow diffusion of pentane into an EtOH solution at *ca.* −20 °C. Crystals were mounted in thin-wall glass capillaries and the crystal system and approximate cell dimensions established by preliminary photographic X-ray examination. The crystal density was measured by flotation. Intensity data were recorded at room temperature using an Enraf-Nonius CAD-4 diffractometer equipped with Mo-Kα radiation and a graphite monochromator. From a crystal 0.60 × 0.30 × 0.15 mm at room temperature were measured 6456 reflections (1.5 < θ < 25°; *h* −14 to 14, *k* −16 to 16, *l* 0–14). Two check reflections showed no decay during the experiment and an empirical ψ-scan absorption correction based on three reflections was applied (transmission: minimum 86.7, maximum 100.0%) as well as Lorentz and polarisation corrections. After data reduction there remained 6324 unique reflections (R_{int} = 0.006) of which 4349 with $F > 3\sigma(F)$ were used in the later refinement.

Crystal data. $C_{65}H_{47}NO_{11}P_3RhRu_3 + nC_5H_{12}$, M_r = 1517.1 + *n*72.1, triclinic, space group *P*1 (no. 1), *a* = 12.244(2), *b* = 13.453(3), *c* = 11.926(3) Å, α = 111.40(2), β = 101.30(2), γ = 70.02(1)°, *U* = 1713.2 Å^3, D_m = 1.56(1) g cm^{-3}, *Z* = 1, D_c = 1.470 (*n* = 0)–1.540 (*n* = 1) g cm^{-3}, *F*(000) = 754 + *n*42, λ(Mo-Kα) = 0.710 69 Å, μ(Mo-Kα) = 9.6 cm^{-1}.

The metal-atom positions were found using the Patterson strategy in SHELXS 86[20] followed by repeated structure-factor and difference electron-density syntheses to locate the remaining non-H atoms. The position of the Rh atom was chosen on the basis of solution ^{13}C-{^1H} NMR data (see later). As the structure refinement proceeded a solvent molecule became apparent in the electron-density maps and was introduced into the model. Although the density measurement favoured one molecule of solvent, the crystallographic evidence suggested only a partial occupancy in the crystal under study, and this model was used. Phenyl H atoms were placed in calculated positions [*d*(CH) = 0.95 Å] with a common refined isotropic thermal parameter; the hydride atoms were not located. Refinement was carried out using SHELX 76[21] and blocked full-matrix least squares with minimisation of $\Sigma w(\Delta)^2$. Least-squares refinement converged to *R* = 0.053 {446 parameters, 4349 reflections, anisotropic (Ru, Rh, P, O, N) and isotropic (C, H) atoms, $w^{-1} = [\sigma^2(F) + 0.0006F^2]$, *R'* = 0.053, maximum Δ/σ = 0.04}. The residual electron density was in the range 0.82 to −0.63 e Å^{-3}, and the site occupancy of the pentane solvate molecule (*n*) refined to 0.60(1). The absolute configuration of the crystal under study was examined by repeating the final calculation for the enantiomorph.[22] The *R* factor increased by a statistically highly significant amount and therefore the configuration of the selected crystal is as reported. The final atomic coordinates are given in Table 1.

Scattering factors for neutral atoms and anomalous dispersion corrections were taken from SHELX 76[21] (P, O, N, C, H)

Table 1 Atomic coordinates for $[N(PPh_3)_2][Ru_3RhH_2(CO)_{11}(PPh_3)]\cdot 0.6C_5H_{12}$

Atom	*x*	*y*	*z*
Ru(1)	0.0000	0.0000	0.0000
Ru(2)	−0.0910(1)	0.1452(1)	0.2188(1)
Ru(3)	−0.0379(1)	0.2416(1)	0.0573(1)
Rh	−0.2184(1)	0.1499(1)	0.0013(1)
P(1)	0.1385(3)	0.2854(3)	0.1172(3)
P(2)	0.4483(3)	−0.2457(3)	−0.5270(3)
P(3)	0.6066(3)	−0.3918(3)	−0.3878(3)
C(1)	−0.3116(13)	0.2509(12)	−0.0790(14)
O(1)	−0.3630(10)	0.3096(12)	−0.1318(13)
C(2)	−0.3213(17)	0.0631(16)	−0.0236(18)
O(2)	−0.3822(13)	0.0127(15)	−0.0360(19)
C(3)	−0.1078(11)	0.0293(11)	−0.1450(14)
O(3)	−0.1226(9)	0.0099(10)	−0.2477(10)
C(4)	0.1396(14)	−0.0898(13)	−0.0664(15)
O(4)	0.2272(11)	−0.1500(12)	−0.1044(14)
C(5)	−0.0480(15)	−0.1223(15)	−0.0105(16)
O(5)	−0.0774(13)	−0.1956(11)	−0.0145(15)
C(6)	0.0738(13)	0.0200(12)	0.1834(14)
O(6)	0.1561(10)	−0.0202(9)	0.2323(10)
C(7)	−0.0549(12)	0.2188(12)	0.3844(14)
O(7)	−0.0334(11)	0.2660(9)	0.4828(10)
C(8)	−0.1479(14)	0.0511(14)	0.2597(15)
O(8)	−0.1841(14)	−0.0055(11)	0.2809(16)
C(9)	−0.2533(14)	0.2504(13)	0.1923(15)
O(9)	−0.3313(10)	0.3207(10)	0.2362(11)
C(10)	−0.0583(13)	0.2460(12)	−0.1014(15)
O(10)	−0.0714(10)	0.2546(11)	−0.1954(10)
C(11)	−0.1430(13)	0.3842(12)	0.1138(13)
O(11)	−0.2083(10)	0.4705(9)	0.1455(12)
N	0.4932(8)	−0.3269(7)	−0.4506(10)
C(21)	0.2318(11)	0.2486(10)	−0.0030(12)
C(22)	0.2313(14)	0.1564(13)	−0.1039(15)
C(23)	0.3024(17)	0.1285(17)	−0.1946(19)
C(24)	0.3734(16)	0.1857(15)	−0.1883(18)
C(25)	0.3801(16)	0.2751(15)	−0.0901(17)
C(26)	0.3048(14)	0.3055(14)	0.0043(16)
C(31)	0.1279(11)	0.4343(11)	0.1920(12)
C(32)	0.1989(13)	0.4710(12)	0.2949(15)
C(33)	0.1892(15)	0.5844(14)	0.3406(16)
C(34)	0.1127(14)	0.6577(14)	0.2869(16)
C(35)	0.0438(15)	0.6222(15)	0.1890(17)
C(36)	0.0488(13)	0.5086(12)	0.1420(14)
C(41)	0.2379(11)	0.2175(11)	0.2206(13)
C(42)	0.3419(14)	0.1329(13)	0.1836(16)
C(43)	0.4129(16)	0.0783(15)	0.2624(17)
C(44)	0.3795(16)	0.1066(15)	0.3766(17)
C(45)	0.2795(14)	0.1847(13)	0.4153(15)
C(46)	0.2077(13)	0.2437(12)	0.3380(14)
C(51)	0.3080(11)	−0.1510(10)	−0.4775(12)
C(52)	0.2481(12)	−0.1775(12)	−0.4100(13)
C(53)	0.1370(14)	−0.1088(13)	−0.3810(15)
C(54)	0.0882(14)	−0.0175(13)	−0.4162(15)
C(55)	0.1445(14)	0.0093(13)	−0.4815(15)
C(56)	0.2554(12)	−0.0571(12)	−0.5154(14)
C(61)	0.4280(11)	−0.3177(10)	−0.6880(12)
C(62)	0.3534(14)	−0.2644(13)	−0.7633(15)
C(63)	0.3464(15)	−0.3193(14)	−0.8868(17)
C(64)	0.4079(15)	−0.4248(15)	−0.9284(18)
C(65)	0.4865(15)	−0.4807(14)	−0.8557(16)
C(66)	0.4932(13)	−0.4284(13)	−0.7333(15)
C(71)	0.5437(11)	−0.1614(10)	−0.5106(12)
C(72)	0.6114(12)	−0.1901(12)	−0.6063(14)
C(73)	0.6899(14)	−0.1307(13)	−0.5856(16)
C(74)	0.6985(13)	−0.0467(13)	−0.4805(15)
C(75)	0.6318(14)	−0.0190(13)	−0.3886(16)
C(76)	0.5524(11)	−0.0809(11)	−0.4067(13)
C(81)	0.7406(12)	−0.3822(11)	−0.4207(13)
C(82)	0.7822(13)	−0.2966(12)	−0.3500(14)
C(83)	0.8793(14)	−0.2820(14)	−0.3796(16)
C(84)	0.9266(17)	−0.3552(16)	−0.4838(18)
C(85)	0.8900(16)	−0.4460(15)	−0.5566(17)
C(86)	0.7937(12)	−0.4576(12)	−0.5230(14)
C(91)	0.5999(12)	−0.3355(12)	−0.2284(14)
C(92)	0.5160(15)	−0.2401(14)	−0.1769(17)
C(93)	0.5125(20)	−0.1951(19)	−0.0480(21)
C(94)	0.5908(22)	−0.2439(21)	0.0238(25)
C(95)	0.6757(28)	−0.3357(26)	−0.0193(31)
C(96)	0.6898(26)	−0.3783(24)	−0.1481(28)
C(101)	0.6145(12)	−0.5373(11)	−0.4366(13)
C(102)	0.7082(15)	−0.6140(14)	−0.4029(16)
C(103)	0.7040(16)	−0.7216(16)	−0.4425(17)
C(104)	0.6163(15)	−0.7559(15)	−0.5098(16)
C(105)	0.5241(15)	−0.6809(14)	−0.5481(16)
C(106)	0.5196(15)	−0.5679(14)	−0.5118(16)
C(111)	0.0160(27)	−0.5211(25)	−0.2120(29)
C(112)	0.1209(27)	−0.4798(25)	−0.2090(30)
C(113)	0.1705(27)	−0.5421(26)	−0.3101(30)
C(114)	0.2276(28)	−0.4584(25)	−0.3328(30)
C(115)	0.3104(29)	−0.4396(25)	−0.2853(30)

The carbon atoms of the phenyl groups are labelled C(*IJ*) where *I* (2–10) indicates the ring and *J* (1–6) the atoms of the *I*th ring. The pentane solvate carbon atoms C(11*K*) (*K* = 1–5) were given a fixed isotropic thermal parameter (0.08 Å^2) and a common refined population [0.6(1)].

and ref. 23 (Ru, Rh). All calculations were carried out on an IBM 3090 computer, using the programs SHELX 76,[21] 86,[20] and ORTEP II.[24]

Additional material available from the Cambridge Crystallographic Data Centre comprises H-atom coordinates, thermal parameters and remaining bond lengths and angles.

Results and Discussion

The reactions described in this paper are presented in Scheme 1 and NMR spectral data for compounds **7** and **8** are given in Tables 2 and 3.

The Reaction of $[Ru_3H_2(CO)_9(\mu_3\text{-COMe})]^-$ *with* $[Rh(CO)_3(PPh_3)_2]^+$.—The anion $[Rh_3H_2(CO)_9(\mu_3\text{-COMe})]^-$ reacts with $[Rh(CO)_3(PPh_3)_2]^+$ in MeOH at −20 °C to form the bimetallic cluster $[Ru_3H_2(CO)_9(\mu_3\text{-COMe})\{Rh(CO)_2(PPh_3)\}]$ **3** in 80% yield. Also formed in this reaction are the compounds $[Ru_3H(CO)_{10}(\mu\text{-COMe})]$ (3%), $[Ru_3H(CO)_9(PPh_3)(\mu\text{-COMe})]$ **4**[25] (5%), $[Ru_3H(CO)_8(PPh_3)_2(\mu\text{-COMe})]$ **5**[25] (1.5%) and $[Ru_3RhH_2(CO)_8(PPh_3)_3(\mu\text{-COMe})]$ **6** (2%). The structures of **3**[15] and **4**[26] have been previously presented.

The ^1H NMR spectrum of compound **5** includes a singlet signal at δ 3.91 due to the Me group of the COMe ligand and a doublet of doublets (*J* = 7, 2 Hz) at δ −13.85 due to the hydride coupling to the two phosphorus nuclei. The $^{31}P\text{-}\{^1H\}$ NMR spectrum (36.23 MHz) shows two signals at δ 38.7 and 38.2 with a P–P coupling of 7 Hz and intensities consistent with an AB spin system. The $^{13}C\text{-}\{^1H\}$ NMR spectrum at room temperature shows some sharp and some broad signals for the CO groups (indicating the presence of exchange processes) along with signals at δ 366.5 and 72.9 from the carbyne and methyl carbon of the μ-COMe ligand. The structure of **5** is likely to be analogous to that of $[Ru_3H(CO)_{10}(\mu\text{-COMe})]$ and **4**. On the basis of the magnitudes of the hydride–phosphorus couplings and steric repulsions it would seem fair to predict that one PPh_3 occupies the same position as that in **4** with the other PPh_3 possibly occupying a site on the Ru atom not involved with the two bridging ligands.

Spectroscopic Characterisation of $[Ru_3H_2(CO)_9(\mu_3\text{-COMe})\{Rh(CO)_2(PPh_3)\}]$ **3**.—The ^1H NMR spectrum for compound **3** contains a singlet signal at δ 4.06 due to the Me group of the COMe ligand and a doublet of doublets (*J* = 1.0, 1.5 Hz) at

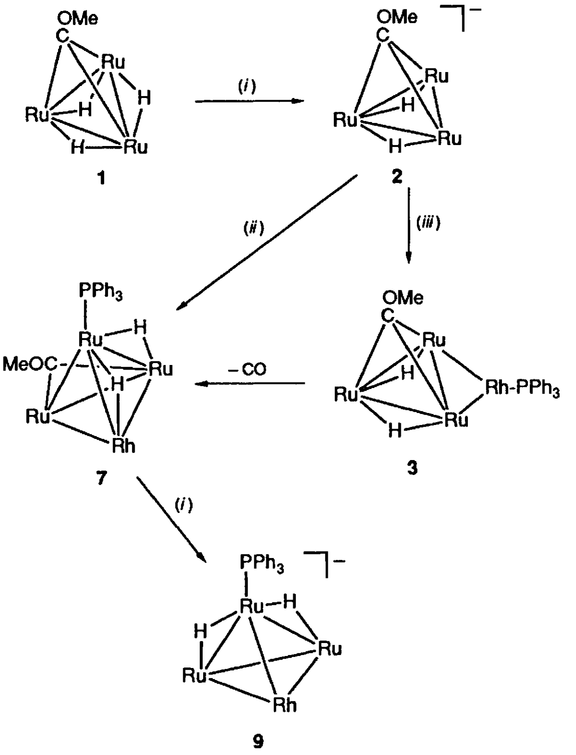

Scheme 1 Main reactions (CO groups omitted). (*i*) $K[BHBu^{s}_{3}]$; (*ii*) $[Rh(CO)(PPh_3)_2Cl]$; (*iii*) $[Rh(CO)_3(PPh_3)_2][PF_6]$

Table 2 NMR data for $[Ru_3RhH_2(CO)_{10}(PPh_3)(\mu\text{-}COMe)]$ **7**

$^{13}C\text{-}\{^1H\}$

Carbon atom	Isomer	$\delta(^{13}C)$ (CDCl$_3$), J/Hz 213	300 K
*C*OMe	**A**	378.7 (s)	379.5 (s)
CO	**A**	215.4 (s, 1 C)	197.8 (s, 8 C)
		207.2 (s, 1 C)	185.8 [d, J(RhC) 66, 2 C]
		199.1 (s, 1 C)	
		197.7 (s, 1 C)	
		197.4 (s, 1 C)	
		193.7 (s, 1 C)	
		189.0 (s, 1 C)	
		186.3 (s, 1 C)	
		185.9 [d, J(RhP) 70, 1 C]	
		185.5 [d, J(RhP) 64, 1 C]	
	B	—	198.5 (d, J 7)
Me	**A**	76.8 (s)	74.1 (s)
	B	74.3 (s)	72.8 (s)

^1H NMR (193 K)

Isomer	δ, J/Hz	Hydride	Edge bridged
A	−17.23 (d of d, J 18, 10)	H_a	Rh–Ru
	−18.52 (d, J 10)	H_b	Ru–Ru
B	−18.23 (d of d, J 16, 7.5)	H_a	
	−18.55 (s)	H_b	

δ −18.02 arising from the metal hydrides coupling with Rh and P. The chemical shift of the Me signal is shifted to slightly higher δ as compared with similar complexes[1] where the equivalent signal lies in the range δ 3.96–3.85.

The $^{31}P\text{-}\{^1H\}$ NMR spectrum shows a doublet signal (J = 139 Hz) at δ 32.2 which is consistent for a Rh-bound PPh_3 and ^1J(RhP) coupling.

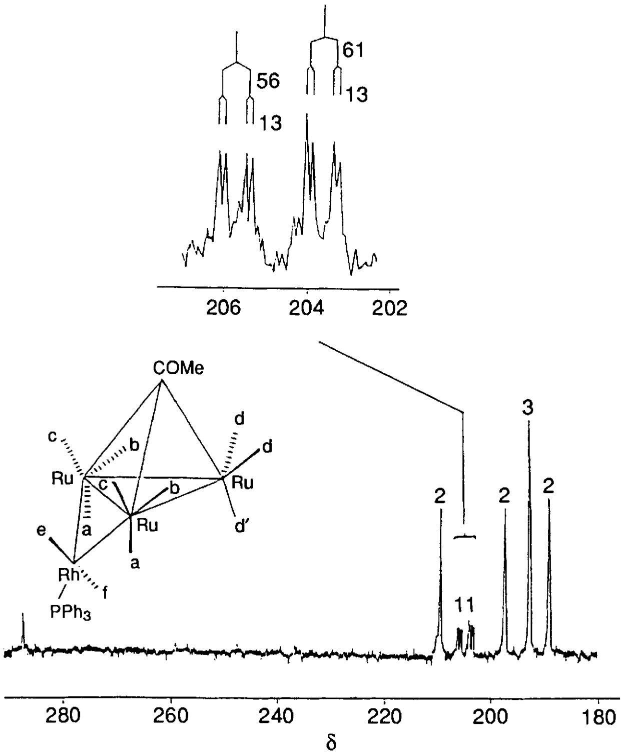

Fig. 1 The $^{13}C\text{-}\{^1H\}$ NMR spectrum of $[Ru_3H_2(CO)_9(\mu_3\text{-}COMe)\{Rh(CO)_2(PPh_3)\}]$ **3** in CD_2Cl_2 at 263 K (90.55 MHz)

The $^{13}C\text{-}\{^1H\}$ NMR spectrum (263 K) is illustrated in Fig. 1 (CO and carbyne signals only) and shows six signals due to terminal CO groups with the indicated relative intensity. The three signals of relative intensity 2 are assigned to the three pairs of CO labelled a, b and c, while the two doublet of doublet signals (relative intensity 1) are assigned to the Rh bound CO groups (labelled e and f) (Fig. 1). The larger couplings are attributed to Rh and the smaller couplings to P. The signal of relative intensity 3 is assigned to the three CO groups labelled d and d′ which are believed to be averaged by rotation about their common Ru atom.[1] The averaging still occurs at temperatures as low as 183 K. The Rh–C couplings of 56 and 61 Hz are typical for terminal CO groups bound to Rh.[27] Fig. 1 also shows the singlet signal of the carbyne carbon of the COMe ligand at δ 287.1.

$[Ru_3RhH_2(CO)_{10}(PPh_3)(\mu\text{-}COMe)]$ **7**.—In solution at room temperature compound **3** rapidly loses CO to form the heterometallic cluster $[Ru_3RhH_2(CO)_{10}(PPh_3)(\mu\text{-}COMe)]$ **7** which has a tetrahedral metal core.[15] In solution, compound **7** exists as two isomers (**A** and **B**) which interconvert slowly on the NMR time-scale at room temperature as shown by ^1H magnetisation-transfer studies. The ratio of these two isomers at room temperature is 2.5:1 (**A** : **B**, $CDCl_3$) and 2.1:1 (**A**:**B**, CD_2Cl_2). The ^1H NMR spectrum (CD_2Cl_2) at room temperature contains two methyl signals (consistent with a μ-COMe ligand) and two hydride signals, one with a triplet structure and the other a doublet of doublets. The effect of cooling on these hydride signals is shown in Fig. 2, with each isomer giving rise to two signals of equal intensity at 193 K as intramolecular H–H exchange is frozen out. The Me signal of each isomer is relatively unaffected by this cooling except for the fact that the signal due to isomer **B** shows some broadening at ≈ 213 K which disappears with further cooling to 183 K.

The $^{31}P\text{-}\{^1H\}$ NMR spectrum at room temperature also shows two signals consistent with the isomeric ratio. This

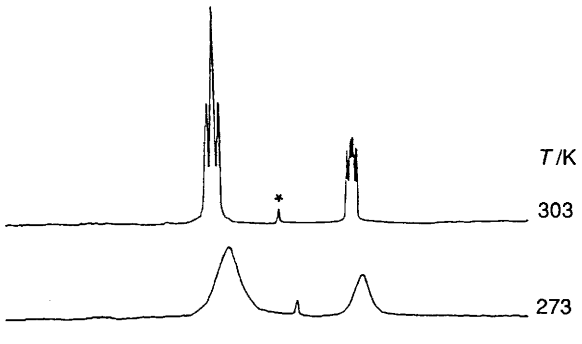

Fig. 2 The variable-temperature ^1H NMR spectra of $[Ru_3RhH_2(CO)_{10}(PPh_3)(\mu\text{-}COMe)]$ **7** for the hydride region in CD_2Cl_2 (360.14 MHz) (* marks a peak from **3** as an impurity)

spectrum clearly shows that the PPh_3 ligand is bound to Rh in isomer **B** [$^1J(RhP) = 140$ Hz] whereas it is bound to Ru in isomer A. The carbonyl signals in the $^{13}C\text{-}\{^1H\}$ NMR spectrum ($CDCl_3$, 213 K) are shown in Fig. 3(*a*) with those due to the major isomer (**A**) clearly identified. The set of signals at highest field (relative intensity 3) is considered to consist of three separate signals; two doublets [$J(RhC) = 70$ and 64 Hz] and a singlet. This assignment is supported by a spectrum at 163 K (CD_2Cl_2–$CHCl_2F$) where splitting of the overlapped signals is just observed. The carbonyl signals of isomer **A** can therefore be interpreted as arising from 10 inequivalent groups, eight bound to Ru and two to Rh. Weaker signals due to the CO groups of isomer **B** are also visible but they are not sufficiently clear to interpret. Only one carbyne signal could be detected which can presumably be attributed to isomer **A**. Fig. 3(*b*) shows the $^{13}C\text{-}\{^1H\}$ NMR carbonyl signals at room temperature with assignments to each isomer which are consistent with signal intensities and isomeric ratio. The signal due to isomer **A** at δ 185.8 is explained as arising from rapid averaging of the two Rh-bound CO. The other signal due to isomer **A** shows no coupling and is four times as intense. It is hence assigned as arising from the other eight CO groups undergoing rapid exchange around the ruthenium centres. Isomer **B** shows just one signal (d, $J = 7$ Hz) corresponding to rapid averaging of all 10 CO with the coupling observed for this signal best explained as an averaged $J(RhC)$. Table 2 summarises the $^{13}C\text{-}\{^1H\}$ NMR data. The NMR results described above provide clear evidence for isomer **A** in solution corresponding to the X-ray crystal structure determined for **7** [see Fig. 4(*a*)].

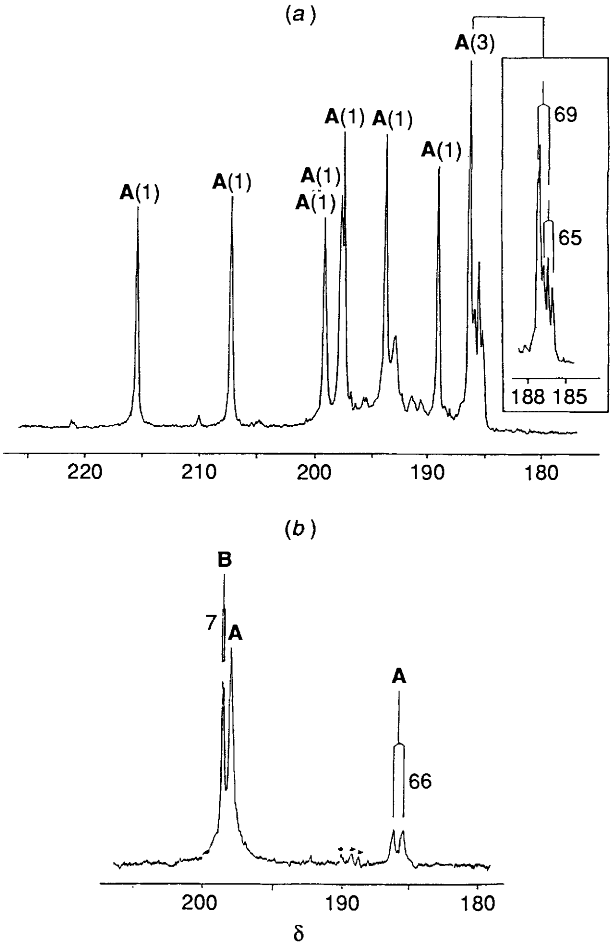

Fig. 3 The $^{13}C\text{-}\{^1H\}$ NMR spectra (90.55 MHz) of $[Ru_3RhH_2(CO)_{10}(PPh_3)(\mu\text{-}COMe)]$ **7** in $CDCl_3$ (*a*) at 213 K (inset 163 K partial spectrum) and (*b*) at room temperature (* marks an impurity)

If the hydride positions on the Ru_3Rh metal core are the same for isomer **B**, H_b would not be expected to show any larger coupling while H_a would show $^1J(RhH)$ and $^2J(PH)$ coupling. This is consistent with the observations and hence assignments for the ^1H NMR hydride signals (193 K) for isomer **B** are as indicated in Table 2. The couplings of 16 and 7.5 Hz are assigned as $^1J(RhH)$ and $^2J(PH)$ respectively. On this basis, the predicted hydride signal for isomer **B** at 303 K (*i.e.* with rapid hydride averaging) is a doublet of doublets with time-averaged couplings of $J(RhH) = 8$ and $J(PH) = 3.75$ Hz. This gives satisfactory agreement with the observed signal and hence it is believed that the hydride positions are indeed the same for both isomers.

Using the NMR evidence described and assuming the two isomers have the same basic structure there are two possible structures for isomer **B** [Fig. 4(*b*)]. Unfortunately, as previously mentioned, low-temperature $^{13}C\text{-}\{^1H\}$ NMR studies of compound **7** do not give any clear information about the individual CO groups in isomer **B**. However, consideration of the magnitude of the RhC couplings observed for the Rh-bound CO groups of isomer A (70 and 64 Hz) suggests that averaging of all the CO groups in the two proposed structures of isomer **B** would give an averaged RhC coupling for **i** of ≈7 Hz and for **ii** of ≈14 Hz, so that **i** is the most likely structure. Hence the most likely process of isomeric interconversion ($\mathbf{A} \longleftrightarrow \mathbf{B}$) appears to be a simple $CO \longleftrightarrow PPh_3$ exchange between sites on the

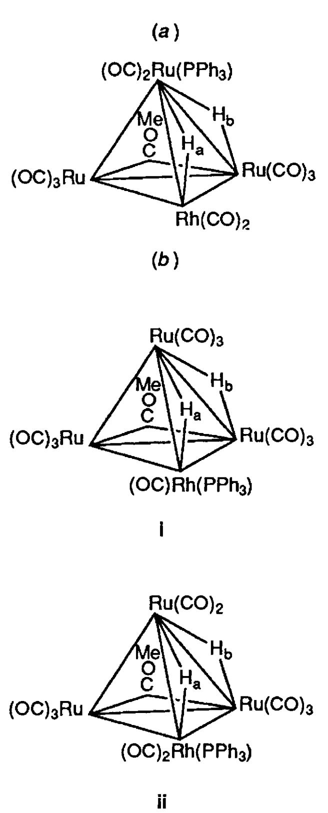

Fig. 4 Proposed structures for isomers **A** (*a*) and **B** (*b*) of $[Ru_3RhH_2(CO)_{10}(PPh_3)(\mu\text{-}COMe)]$ **7**

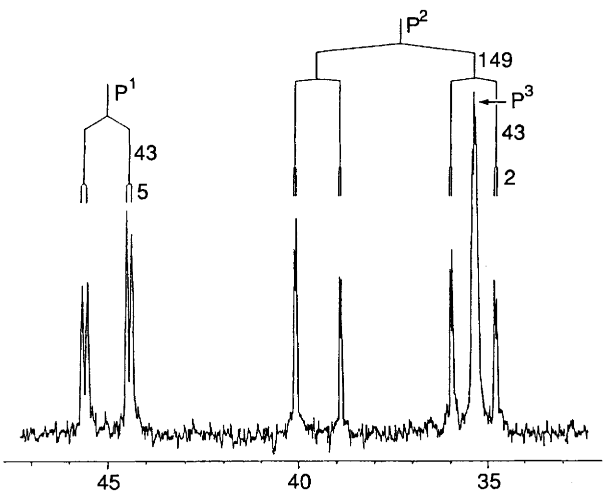

Fig. 5 The $^{31}P\text{-}\{^1H\}$ NMR spectrum of $[Ru_3RhH_2(CO)_8(PPh_3)_3(\mu\text{-}COMe)]$ **6** (room temperature, $CDCl_3$, 36.23 MHz)

Rh atom and the Ru atom not bound to COMe. This is an unusual process, but internuclear phosphine exchange has been observed in $[Pt_3(\mu_3\text{-}CO)(dppm)_3(PR_3)]^{2+}$ species (dppm = $Ph_2PCH_2PPh_2$).[28]

The formation of compound **7** from **3** involves the loss of a CO ligand with generation of a Ru–Rh bond. It is not reversible. Compound **7** reacts rapidly with CO and after about 30 min under CO a thf solution of **7** consists of a large number of products (TLC shows more than six) with the major decomposition product identified as $[Ru_3H(CO)_{10}(\mu\text{-}COMe)]$ (*ca.* 20%).

The Heterometallic Cluster $[Ru_3RhH_2(CO)_8(PPh_3)_3(\mu\text{-}COMe)]$ **6**.—Also produced in the synthesis of compound **3** is another heterometallic cluster *i.e.* $[Ru_3RhH_2(CO)_8(PPh_3)_3(\mu\text{-}COMe)]$ **6**. The ^1H NMR spectrum of **6** shows phenyl signals for three PPh_3 groups along with a singlet at δ 4.44 due to the Me group of the COMe ligand and two multiplet hydride signals at δ −15.79 and −17.27. The signal at δ −15.79 is best explained by an overlapping doublet of triplets of triplets (*J* = 19.5, 9, 2 Hz) with the largest two couplings consistent with $^1J(RhH)$ and $^2J(PH)$ couplings respectively. The coupling of 2 Hz is likely to be due to $^2J(HH)$ or a small PH coupling. The other multiplet has a broad triplet-based structure.

The $^{13}C\text{-}\{^1H\}$ NMR spectrum shows, in particular, a singlet signal at δ 391.1 for the carbyne of the μ-bridging COMe ligand and signals due to eight inequivalent CO groups, of which one is bridging (δ 230.1) and one is bound to Rh [*J*(RhC) = 72 Hz].

The $^{31}P\text{-}\{^1H\}$ NMR spectrum is shown in Fig. 5 and consists of signals arising from three different PPh_3 ligands with phosphorus atoms P^1, P^2 and P^3 such that: (*a*) P^1 shares a P–P coupling of 43 Hz with P^2 and shows a smaller coupling (5 Hz) attributed to ^2J coupling to Rh; (*b*) P^2 exhibits $^1J(RhP)$ coupling of 149 Hz, P–P coupling to P^1 of 43 Hz and a small coupling of 2 Hz believed to be P–P coupling to P^3; and (*c*) P^3 shows small couplings to at least two other nuclei of the order of a few Hz which are not quite fully resolved.

The predicted structure of compound **6** is based on that determined for the related $[Ru_3RhH_2(CO)_{10}(PPh_3)(\mu\text{-}COMe)]$ **7** and is believed to consist of a tetrahedral metal core with two bridging hydrides, seven terminal CO, one bridging CO, three PPh_3 ligands and the COMe ligand bridging a Ru–Ru bond. The bridging CO is thought to bridge a Ru–Ru edge. Although the ^{13}C NMR signal for this CO shows coupling, its magnitude (12 Hz) is too low for a RhC coupling if a Rh–Ru edge were bridged. The ^{31}P NMR spectrum shows that two PPh_3 ligands are bound to Ru and one to Rh with P^1 and P^2 transoid (as they show a large P–P coupling).

The Reaction of $[Ru_3H_2(CO)_9(\mu_3\text{-}COMe)]^-$ *with* $[Rh(CO)(PPh_3)_2Cl]$.—The anion $[Ru_3H_2(CO)_9(\mu_3\text{-}COMe)]^-$ reacts with $[Rh(CO)(PPh_3)_2Cl]$ in thf at room temperature to form the bimetallic cluster $[Ru_3RhH_2(CO)_9(PPh_3)_2(\mu\text{-}COMe)]$ **8** in 20% yield. Also formed in this reaction is $[Ru_3RhH_2(CO)_{10}(PPh_3)(\mu\text{-}COMe)]$ **7** (20% yield). Complex **8** is believed to have a structure similar to that of **7** but with one CO substituted by PPh_3. In solution in CD_2Cl_2 at room temperature, **8** appears to exist as four isomers (**a**, **b**, **c** and **d**) in the ratios 1:0.5:0.15:0.02 respectively. This is illustrated by the ^1H NMR spectrum at room temperature which shows four singlet signals due to the Me group of the COMe ligand of each isomer at δ 4.76, 4.34, 4.29 and 4.11. Low-temperature ^1H NMR (CD_2Cl_2) methyl signals of **8** indicate that isomer **b** at 298 K results from the averaging of two isomers (**b′** and **b″**). The ratio of the five isomers at 213 K (CD_2Cl_2) is **a**:**b′**:**b″**:**c**:**d** = 1:0.33:0.20:0.10:0.02. Fig. 6 shows the corresponding hydride signals at 273 and 213 K respectively, with their assignment to each isomer. These two spectra clearly show that the two hydride ligands are inequivalent in all isomers and hence that no rapid hydride exchange is occurring at either 213 or 273 K. Table 3 summarises the ^1H NMR data at 213 and 273 K with the structure of the hydride signals (except for the signal $\mathbf{a}_1$ at 273 K) explained in terms of overlapping couplings. The signal $\mathbf{a}_1$ at 273 K has the basic structure expected for an overlapping doublet of triplets with coupling constants of 19 and 9 Hz but close inspection shows each of the main branches to have a triplet structure ($J \approx 2$ Hz) which cannot be accounted for by four spin $\frac{1}{2}$ nuclei.

Proton magnetisation-transfer NMR studies at 273 K (CD_2Cl_2) provide clear evidence for an isomeric mixture as opposed to a mixture of inseparable compounds and transfers corresponding to the isomer interconversion matrix shown in Scheme 2 are observed. Moreover, referring to the hydride signals at 273 K the specific interconversions in Scheme 3 are observed which show that the isomer interconversions detected

Table 3 NMR data for [$Ru_3RhH_2(CO)_9(PPh_3)_2(\mu$-COMe)] **8**

(*a*) ^1H

Isomer	*T*/K	δ (^1H) (CD_2Cl_2),[a] *J*/Hz Me	μ-H
a	213	4.70	−16.45 (br, 1 H)
			−18.29 (d, *J* 10, 1 H)
	273	4.75	−16.48 (m, 1 H)
			−18.18 (d, *J* 12, 1 H)
b	273	4.26	−17.38 (d of t, *J* 14.5, 7.5)
			−18.1 (vbr, 1 H)
b′	213	4.45	−17.38 (m, 1 H)
			−18.52 (d, *J* 10, 1 H)
b″	213	3.77	−17.19 (d, *J* 11, 1 H)
			−17.61 (m, 1 H)
c	213	4.28	−16.83 (d of d of t, *J* 18, 13, 2, 1 H)
			≈ −17.6 (m, 1 H)
	273	4.32	−16.71 (d of d of t, *J* 18.5, 14, 2.5, 1 H)
			−17.49 (d of d of d, *J* 10, 8, 2.5, 1 H)
d	213	4.10	≈ −17.4 (hidden by signal due to **b′**)
			−19.47 (d of t, *J* 15, 3.5)
	273	4.11	−17.23 (d, *J* 6, 1 H)
			−19.30 (d of t, *J* 15, 3, 1 H)

(*b*) $^{13}C-\{^1H\}$

Isomer	*T*/K	δ(^{13}C) (CD_2Cl_2)[b]
a	213	74.9 (s)
	298	74.0 (s)
b	298	71.9 (s)
b′	213	74.4 (s)
b″	213	70.2 (s)
c	213	73.8 (s)
	298	72.8 (s)
d	213	68.2 (s)
	298	68.0 (s)

(c) $^{31}P-\{^1H\}$

Isomer	*T*/K	δ(^{31}P),[c] *J*/Hz
a	183	37.9 (s, 1 P)
		40.8 [br d, ^1J(RhP) 148, 1 P]
	298	38.1 [d of d, ^2J(RhP) 3, *J*(PP) 2, 1 P]
		39.0 [d of d, ^1J(RhP) 150, *J*(PP) 2, 1 P]
b	298	35.9 [d of d, ^1J(RhP) 141, *J*(PP) 26, 1 P]
		47.2 [d of d, *J*(PP) 26, ^2J(RhP) 5, 1 P]
b′	183	40.8 [d of d, ^1J(RhP) 143, *J*(PP) 38, 1 P]
		49.3 [d of d, *J*(PP) 38, ^2J(RhP) 4, 1 P]
b″	183	29.5 [d, ^1J(RhP) 135, 1 P]
		46.3 [d, ^2J(RhP) 7, 1 P]
c	183	36.8 (s, 1 P)
		47.4 (d, *J* 2, 1 P)
	298	37.4 (s, 1 P)
		47.4 (d, *J* 1, 1 P)[d]

[a] Phenyl signals omitted. [b] Methyl-carbon signals only, solvents CD_2Cl_2 (213 K) and $CDCl_3$ (298 K). [c] Spectra recorded at 36.23 MHz in CD_2Cl_2 (183 K) and $CDCl_3$ (298 K). [d] An additional coupling (≈2 Hz) also appears to be present but this signal is obscured by that of isomer **b**.

$$\begin{tikzcd}
\mathbf{a} \arrow[r, leftrightarrow] \arrow[d, leftrightarrow] & \mathbf{b} \arrow[d, leftrightarrow] \arrow[dl, leftrightarrow] \\
\mathbf{c} & \mathbf{d}
\end{tikzcd}$$

Scheme 2

$\mathbf{a}_2 \longleftrightarrow \mathbf{b}_1, \mathbf{b}_2$
$\mathbf{c}_1 \longleftrightarrow \mathbf{a}_1, \mathbf{a}_2$
$\mathbf{c}_2 \longleftrightarrow \mathbf{b}_1, \mathbf{b}_2$
$\mathbf{d}_1 \longleftrightarrow \mathbf{b}_1, \mathbf{b}_2$

Scheme 3

lead to scrambling of the hydrides. Transfers are also seen for $\mathbf{a}_1 \longleftrightarrow \mathbf{a}_2$ and $\mathbf{b}_1 \longleftrightarrow \mathbf{b}_2$, probably due to slow H ⟷ H exchange. Irradiation of $\mathbf{b}_2$ was not attempted due to its broad nature.

The $^{13}C-\{^1H\}$ NMR spectrum (CD_2Cl_2) at 213 K shows five methyl signals which are consistent with the ratios of **a**, **b′**, **b″**, **c** and **d**. The same spectrum also shows four singlet signals at low field (δ 389.4, 385.8, 380.0 and 314.9). The three at lowest field are consistent with the carbyne atom of a μ-COMe ligand and that at δ 385.8 is the most intense, while that at δ 314.9 also encompasses a μ_3-COMe shift range a little lower than might be expected. The carbonyl region of the spectrum shows a very large number of signals, some sharp and some broad, between δ 234 and 184. A $^{13}C-\{^1H\}$ NMR spectrum ($CDCl_3$) at 298 K showed, in particular, four methyl signals (as expected) but only one carbyne signal at δ 387.0. Table 3 includes the ^{13}C NMR methyl-carbon chemical shifts for the isomers of **8**.

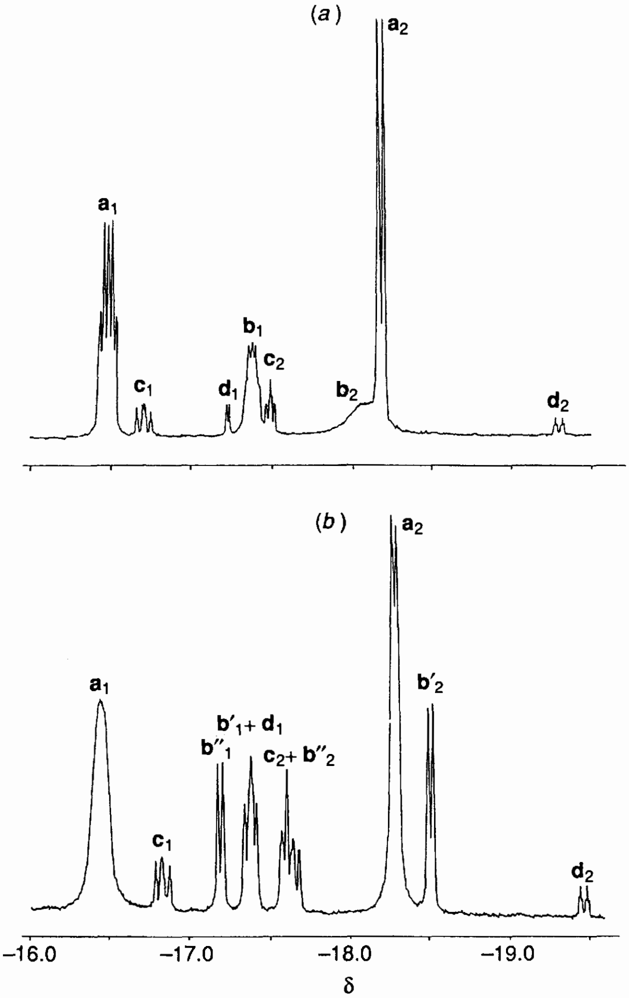

Fig. 6 The partial ^1H NMR spectra (hydride region) of [$Ru_3RhH_2(CO)_9(PPh_3)_2(\mu$-COMe)] **8** ($CD_2Cl_2$, 360.14 MHz) at 273 (*a*) and 213 K (*b*)

The $^{31}P-\{^1H\}$ NMR spectrum at 183 K is illustrated in Fig. 7(*a*) and the integration ratios allow assignment of each signal to its respective isomer. The signals due to isomer **d** were not unambiguously identified due to its very low abundance; there is a weak signal at δ 24.6 [*J*(RhP) = 139 Hz] which, if due to **d**, shows one PPh_3 to be bound to Rh. The chemical shifts, coupling constants and assignments are summarised in Table 3. Fig. 7(*b*) shows the $^{31}P-\{^1H\}$ NMR spectrum at room temperature along with the respective isomeric assignments. Signals due to the minor isomer, **d**, were not observed in the room-temperature spectra.

Using the observed couplings for the ^{31}P NMR signals of the isomers of compound **8** the following conclusions can be made as to: (*i*) which metal the PPh_3 ligands are bound [from the *J*(RhP) values], and (*ii*) whether the two PPh_3 in each isomer are mutually cisoid or transoid [from the *J*(PP) values].

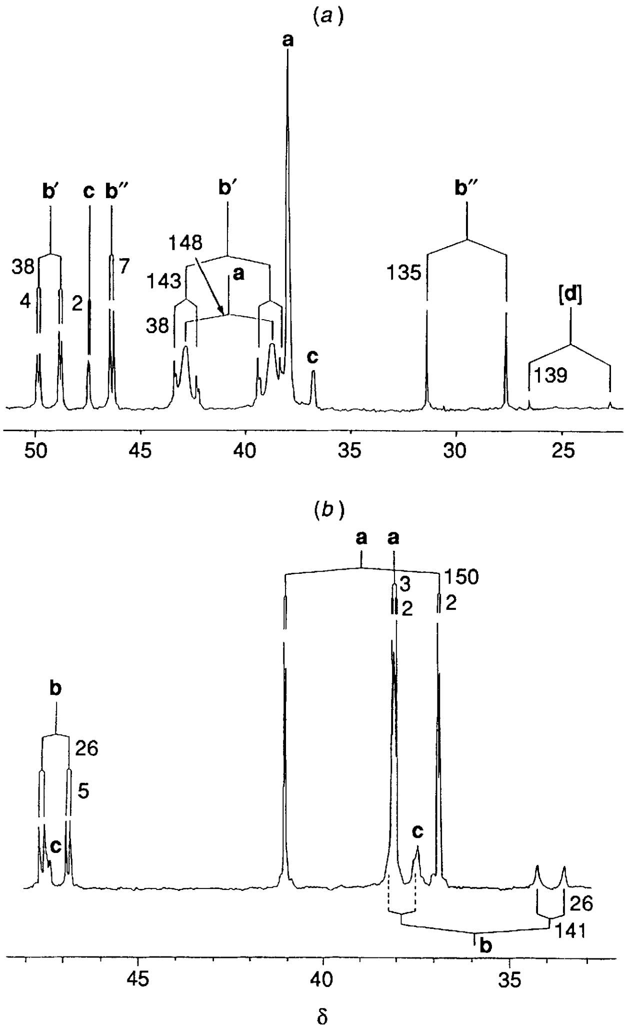

Fig. 7 The ^{31}P-{^{1}H} NMR spectrum of [$Ru_3RhH_2(CO)_9(PPh_3)_2(\mu$-COMe)] **8** ($CD_2Cl_2$, 36.23 MHz) at 183 K (*a*) and room temperature (*b*)

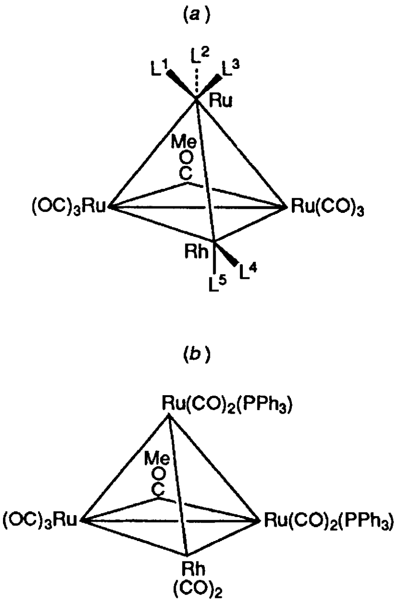

Fig. 8 The proposed structures for the isomers of [$Ru_3RhH_2(CO)_9(PPh_3)_2(\mu$-COMe)] **8**: (*a*) Isomers **a** (cisoid PPh_3 groups at L^5 and L^1, L^2 or L^3, or L^4 and L^1 or L^3), **b′** (transoid PPh_3 groups at L^4 and L^2) and **b″** (cisoid PPh_3 groups with the same options as isomer **a**); (*b*) isomer **c** (PPh_3 groups cisoid)

Due to the complexity of the isomeric system for compound **8** it is not possible unambiguously to assign structures for each isomer. However, there is sufficient evidence to suggest that the structures of these isomers are based on that determined for [$Ru_3RhH_2(CO)_{10}(PPh_3)(\mu$-COMe)] **7** *i.e.* a tetrahedral metal core with the COMe ligand edge-bridging a Ru–Ru bond. As the ^{13}C NMR spectrum (213 K) shows some carbonyl signals at relatively low field (*e.g.* δ 223, 227) it would appear that bridging CO groups are present in the isomeric mixture of **8** which differs from that observed for **7**. However, **7** does have two semi-bridging CO groups and the basic arrangement of ligands for **7** and **8** is likely to be similar. Assuming that for all isomers one PPh_3 ligand is bound to the Ru atom not involved in COMe bonding (as observed for **7**) structures are tentatively proposed for isomers **a**, **b′**, **b″** and **c**. Fig. 8 shows the general structure predicted for the isomers.

Isomer	PPh_3 bound to Ru	Rh	PPh_3 geometry
a	1	1	cisoid
b′	1	1	transoid
b″	1	1	cisoid
c	2	0	cisoid

The X-Ray Structure of [$N(PPh_3)_2$][$Ru_3RhH_2(CO)_{11}(PPh_3)$]$\cdot 0.6C_5H_{12}$.—Complex **7** rapidly reacts with K[$BHBu^s_3$] in thf to generate the anion [$Ru_3RhH_2(CO)_{11}(PPh_3)$]$^-$ which was isolated as the [$N(PPh_3)_2$]$^+$ salt. The crystal structure contains discrete anions, [$N(PPh_3)_2$]$^+$ cations, and pentane solvent molecules and an anion is shown in Fig. 9. The Rh atom was distinguished from Ru by solution ^{13}C-{^{1}H} NMR spectroscopy which showed consistent molecular symmetry and couplings. Selected bond lengths and angles are given in Table 4. The anion adopts a tetrahedral metal core with an apical Ru atom [Ru(3)] co-ordinated by two CO ligands and a PPh_3 ligand, and a basal $Ru_2Rh(CO)_9$ fragment where each metal atom is co-ordinated to two terminal CO groups and each metal–metal bond is bridged by a CO. The two hydride ligands are believed to bridge the Ru(1)–Ru(3) [2.953(2) Å] and Ru(2)–Ru(3) [2.950(3) Å] bonds which are significantly longer than the other Ru–Ru bonds in the molecule [2.743(1)–2.792(1) Å]. These positions are also consistent with NMR studies and the M–M–C bond angles which show that C(4)–O(4) and C(7)–O(7) are pushed further away from the metal core than C(1)–O(1) [Ru(3)–Ru(2)–C(7) 112.4(6), Ru(3)–Ru(1)–C(4) 114.1(6) and Ru(3)–Rh–C(1) 93.1(6)°]. The PPh_3 ligand is positioned over a face of the tetrahedron such that it sits between the two hydride-bridged edges [P(1)–Ru(3)–Ru(1) 111.1(1) and P(1)–Ru(3)–Ru(2) 112.9(1)°] and is bent further away from the metal core than the two CO ligands bound to Ru(3) (mean C–Ru–Ru/Rh bond angle 93.5°). This is very similar to the PPh_3 orientation for compound **7** and hence it is believed that the two hydride ligands of **9** effectively occupy the space on the Ru(1)–Ru(2)–Ru(3) triangular face created by the steric demands of the bulky phosphine ligand.

The metal–metal bond lengths are unexceptional with the non-hydride-bridged bonds [2.76 Å (av.)] similar to the mean Rh–Rh distance observed in [$Rh_4(CO)_{12}$] (2.73 Å).[29] The Ru/Rh–C and C–O bond lengths are normal with C(6)–O(6) symmetrically bridging Ru(1)–Ru(2) (mean Ru–C 2.14 Å), and C(3)–O(3) and C(9)–O(9) asymmetrically bridging Ru(1)–Rh and Ru(2)–Rh such that the Ru–C bonds [2.03(2) and 2.05(2) Å] are significantly shorter than the Rh–C bonds [2.21(1) and 2.22(2) Å]. The stronger Ru–C bonding for these two CO groups is presumably required to prevent electron deficiency at the Ru(1) and Ru(2) centres.

The terminal CO groups have a mean Ru/Rh–C–O angle of

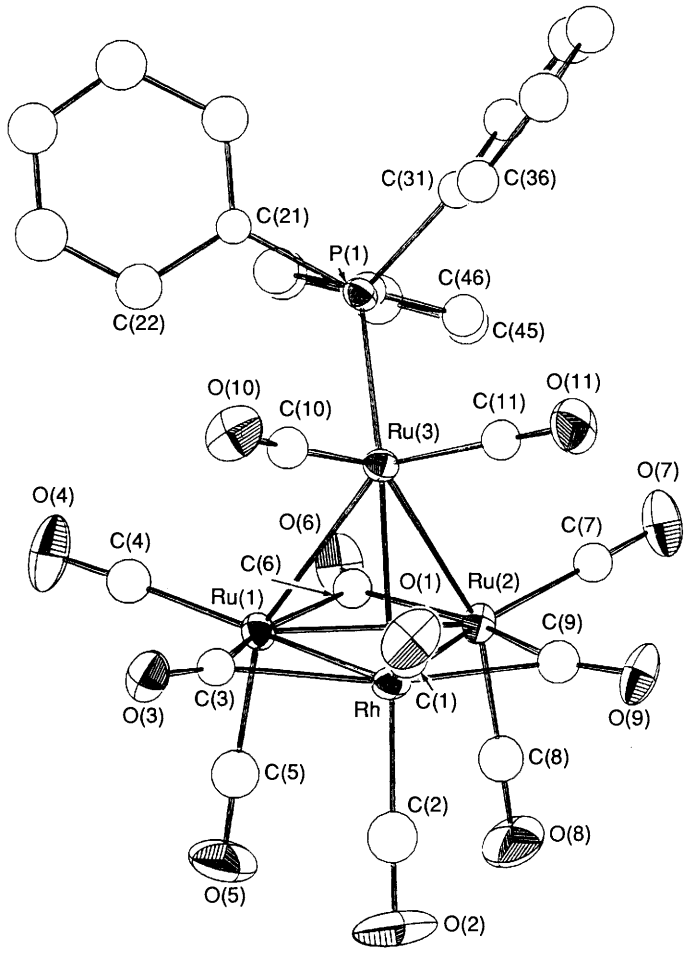

Fig. 9 The molecular structure of the anion in $[N(PPh_3)_2]$-$[Ru_3RhH_2(CO)_{11}(PPh_3)]\cdot 0.6C_5H_{12}$. Hydride H atoms were not located. Phenyl H atoms are excluded for clarity and the thermal ellipsoids are drawn at the 25% probability level

178° while the two asymmetrically bridging CO groups have smaller Rh–C–O bond angles [131(1) and 133(1)°] than the corresponding Ru–C–O angles [148(1) and 147(1)°] (as would be expected). The symmetrically bridging CO makes Ru–C–O angles of 138(1) and 141(1)°. The N–P bond lengths in the $[N(PPh_3)_2]^+$ cation are 1.56(1) and 1.58(1) Å and the P–N–P bond angle is 143.3(9)°.

The anion has an analogous structure to that of $[Rh_4(CO)_{12}]$,[27] $[Ru_2Rh_2H_2(CO)_{12}]$,[8] and $[RuRh_3H(CO)_{12}]$[6] which show characteristic tetrahedral metal cores with a basal $M_3(CO)_6(\mu\text{-}CO)_3$ fragment (M = Ru or Rh) and an apical $M(CO)_3$ unit. Triphenylphosphine-substituted derivatives of these three examples have also been reported, *i.e.* $[Rh_4(CO)_{11}(PPh_3)]$,[27] $[Rh_4(CO)_{10}(PPh_3)_2]$,[30] $[Ru_2Rh_2H_2(CO)_{11}(PPh_3)]$,[31] and $[RuRh_3H(CO)_{10}(PPh_3)_2]$,[6] and in contrast to **9** the phosphines in these clusters occupy positions on the basal fragment.

Spectroscopic Characterisation of $[N(PPh_3)_2][Ru_3RhH_2(CO)_{11}(PPh_3)]$ **9**.—The ^1H NMR spectrum of compound **9** includes a doublet hydride signal (J = 10 Hz) at δ −19.42. The magnitude of this coupling is too small for a $^1J(RhH)$ coupling (typically ≈ 17 Hz) and indicates a $^2J(PH)$ interaction. The $^{13}C\text{-}\{^1H\}$ NMR carbonyl signals (CD_2Cl_2, 183 K) are illustrated in Fig. 10. This is consistent with the symmetry expected for the molecule from the X-ray structure. The two signals at low field are consistent for the bridging CO groups with the signal of relative intensity 1 assigned to the CO labelled d and the signal with relative intensity 2 assigned to the CO groups labelled e. The RhC coupling of 22 Hz observed for the CO groups labelled e is similar to that reported[8] for two CO in $[Ru_2Rh_2H_2(CO)_{12}]$ which asymmetrically bridge Ru–Rh bonds in the same fashion as observed for **9**. The two high-field signals (relative intensity 1) both show typical $^1J(RhC)$ couplings for terminal CO groups bound to Rh and hence arise from the CO groups labelled f and g. Of these signals the one at δ 183.0 shows additional PC coupling of 18 Hz and hence

Table 4 Selected bond lengths (Å) and angles (°) for $[N(PPh_3)_2]$-$[Ru_3RhH_2(CO)_{11}(PPh_3)]\cdot 0.6C_5H_{12}$

Ru(1)–Ru(2)	2.792(1)	Ru(3)–P(1)	2.341(4)
Ru(1)–Ru(3)	2.953(2)		
Ru(1)–Rh	2.743(1)	N–P(2)	1.56(1)
Ru(2)–Ru(3)	2.950(3)	N–P(3)	1.58(1)
Ru(2)–Rh	2.762(2)		
Ru(3)–Rh	2.745(2)	P(2) ··· P(3)	2.982(5)
Rh–C(1)	1.88(2)	Ru(1)–C(6)	2.15(2)
Rh–C(2)	1.91(2)	Ru(2)–C(6)	2.14(1)
Rh–C(3)	2.21(1)	Ru(2)–C(7)	1.90(1)
Rh–C(9)	2.22(2)	Ru(2)–C(8)	1.87(2)
Ru(1)–C(3)	2.03(2)	Ru(2)–C(9)	2.05(2)
Ru(1)–C(4)	1.85(2)	Ru(3)–C(10)	1.88(2)
Ru(1)–C(5)	1.88(2)	Ru(3)–C(11)	1.87(1)
P(1)–C(21)	1.83(2)	P(2)–C(71)	1.83(2)
P(1)–C(31)	1.84(1)	P(3)–C(81)	1.81(2)
P(1)–C(41)	1.82(1)	P(3)–C(91)	1.78(2)
P(2)–C(51)	1.81(1)	P(3)–C(101)	1.80(1)
P(2)–C(61)	1.82(1)		

	Minimum	Maximum
C–C (phenyl)	1.32(2)	1.45(3)
C–O	1.12(3)	1.16(2)
C–H (phenyl)	fixed 0.95	

Ru(1)–Ru(2)–Ru(3)	61.8(1)	Rh–Ru(2)–Ru(3)	57.3(1)
Ru(2)–Ru(3)–Ru(1)	56.5(1)	Ru(2)–Ru(3)–Rh	57.9(1)
Ru(3)–Ru(1)–Ru(2)	61.7(1)	Ru(3)–Rh–Ru(2)	64.8(1)
Rh–Ru(1)–Ru(3)	57.5(1)	Rh–Ru(2)–Ru(1)	59.2(1)
Ru(1)–Ru(3)–Rh	57.4(1)	Ru(2)–Ru(1)–Rh	59.9(1)
Ru(3)–Rh–Ru(1)	65.1(1)	Ru(1)–Rh–Ru(2)	61.0(1)
Ru(3)–P(1)–C(21)	116.4(4)	P(1)–Ru(3)–Ru(1)	111.1(1)
Ru(3)–P(1)–C(31)	116.4(4)	P(1)–Ru(3)–Rh	167.5(1)
Ru(3)–P(1)–C(41)	115.3(6)	P(1)–Ru(3)–Ru(2)	112.9(1)
P(2)–N–P(3)	143.3(9)		

	Minimum	Maximum
Ru/Rh–C–O (terminal)	176(1)	179(2)
Ru/Rh–C–O (bridging)	131(1)	148(1)
C–P–C	101.0(7)	109.0(8)
N–P–C	107.8(7)	114.1(6)
C–C–C (phenyl)	116(2)	125(2)

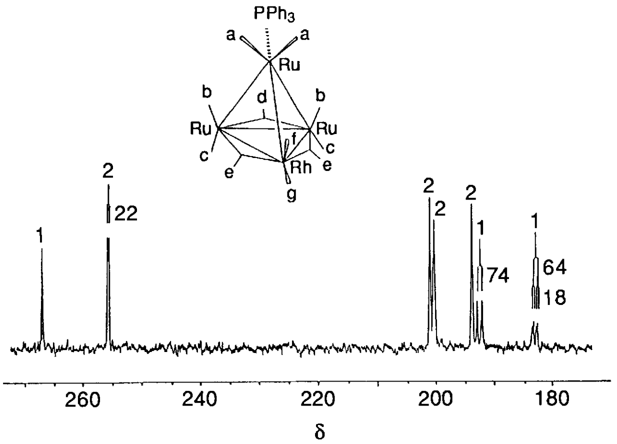

Fig. 10 The $^{13}C\text{-}\{^1H\}$ NMR spectrum (90.55 MHz) of $[N(PPh_3)_2]$-$[Ru_3RhH_2(CO)_{11}(PPh_3)]$ **9** in CD_2Cl_2 at 183 K

can be assigned to the CO labelled g which is transoid to the PPh_3 ligand. The other high-field signal is hence due to the CO labelled f. The remaining three singlet signals (relative intensity 2) are due to the three pairs of CO groups labelled a, b and c.

The Reaction of $[Ru_3RhH_2(CO)_{10}(PPh_3)(\mu\text{-COMe})]$ **7** *with* $K[BHBu^s_3]$.—The reaction of compound **7** with $K[BHBu^s_3]$ in thf solution to form the anion $[Ru_3RhH_2(CO)_{11}(PPh_3)]^-$ seems likely to involve 'H^-' attack at the methyl group of the μ-COMe ligand resulting in abstraction of Me^+ and formation of a CO ligand. Such reactivity for an edge-bridging COMe ligand seems reasonable when considering the bonding within the ligand, *i.e.* with the C(carbyne)–O bond having some multiple-bond character due to partial π bonding.

In contrast, the reactivity of $[Ru_3H(CO)_{10}(\mu\text{-COMe})]$ with an equimolar quantity of $K[BHBu^s_3]$ in thf has also been studied and NMR and IR results show the major product is the anion $[Ru_3H_2(CO)_9(\mu_3\text{-COMe})]^-$. The ^1H NMR spectrum of the reaction solution at 223 K (after addition of $K[BHBu^s_3]$ at ≈183 K and transfer to the NMR instrument without warming), although complicated, shows three broad signals due to formyl protons (δ 14.1, 13.4 and 13.3) which disappear on warming. Hence the reaction is best described as in Scheme 4.

$$[Ru_3H(\mu\text{-COMe})(CO)_9\text{–C=O}] \xrightarrow[\text{thf}]{H^-}$$

$$[Ru_3H(\mu\text{-COMe})(CO)_9\text{–C(=O)–H}]^-$$

$$\Big\downarrow {-CO}$$

$$[Ru_3H_2(CO)_9(\mu_3\text{-COMe})]^-$$

Scheme 4

Similar attack of 'H^-' on CO leading to formation of a formyl group is also proposed for the reaction of $[Ru_3(CO)_{10}(\mu\text{-}Ph_2ECH_2EPh_2)]$ (E = P or As) with $K[BHBu^s_3]$–thf.[32] Reduction of $[Ru_3H(CO)_{10}(\mu\text{-COMe})]$ can also be achieved with molecular hydrogen which results in formation of $[Ru_3H_3(CO)_9(\mu_3\text{-COMe})]$ **1**.[18]

Possible explanations for the contrasting reactivity of the μ-COMe ligand in compound **7** compared to $[Ru_3H(CO)_{10}(\mu\text{-COMe})]$ are: (*i*) stronger C(carbyne)–O bonding and weaker O–CH_3 bonding, and/or (*ii*) greater stability of the anionic product derived from loss of Me. Comparison of the C(carbyne)–O bond length determined for isomer **A** of **7** with $[Ru_3H(CO)_{10}(\mu\text{-COMe})]$[17] does show it to be slightly shorter [1.28(1) and 1.305(5) Å respectively] with the O–CH_3 bond length being little changed [1.47(1) and 1.467(8) Å respectively]. The reactivity of both **7** and $[Ru_3H(CO)_{10}(\mu\text{-COMe})]$ with $K[BHBu^s_3]$ can be contrasted with that of $[Ru_3H_3(CO)_9(\mu_3\text{-COMe})]$ **1** with $K[BHBu^s_3]$–thf where proton loss is observed to form the anion $[Ru_3H_2(CO)_9(\mu_3\text{-COMe})]^-$. Proton loss for **7** with $K[BHBu^s_3]$–thf would be expected to form the anion $[Ru_3RhH(CO)_{10}(PPh_3)(COMe)]^-$ and although this anion has not been isolated and characterised ^1H and $^{31}P\text{-}\{^1H\}$ NMR studies of the reaction do show that products in addition to the major product, $[Ru_3RhH_2(CO)_{11}(PPh_3)]^-$, are formed. Specific evidence for the existence of the alternative anion comes from treatment of the reaction mixture derived from **7** and $K[BHBu^s_3]$ with $[Au(PPh_3)Cl]$ which leads to generation of $[Ru_3RhAuH(CO)_{10}(PPh_3)_2(\mu_3\text{-COMe})]$.[33] Bearing in mind the fact that **7** exists as two isomers in solution, it seems reasonable to suggest that each of these isomers shows different reactivity with $K[BHBu^s_3]$ resulting in each forming a different anion. The structural evidence derived from this study is consistent with the pathways (1) and (2).

$$\underset{\text{(isomer A)}}{[Ru_3RhH_2(CO)_{10}(PPh_3)(\mu\text{-COMe})]} \xrightarrow[\text{thf}]{K[BHBu^s_3]} [Ru_3RhH_2(CO)_{11}(PPh_3)]^- \quad (1)$$

$$\underset{\text{(isomer B)}}{[Ru_3RhH_2(CO)_{10}(PPh_3)(\mu\text{-COMe})]} \xrightarrow[\text{thf}]{K[BHBu^s_3]} [Ru_3RhH(CO)_{10}(PPh_3)(COMe)]^- \quad (2)$$

Acknowledgements

We thank the SERC for support (to P. M. S.) and access to the X-ray service, Professor M. B. Hursthouse for the X-ray data collection, Dr. G. J. Langley for the mass spectra, Mrs. J. M. Street for the two-dimensional NMR spectra, Dr. W. Levason for the elemental analyses, and Johnson Matthey for the loan of ruthenium salts. We thank a referee for helpful comments.

References

1 J. Evans, P. M. Stroud and M. Webster, *Organometallics*, 1989, **8**, 1270.
2 L. W. Bateman, M. Green, K. A. Mead, R. M. Mills, I. D. Salter, F. G. A. Stone and P. Woodward, *J. Chem. Soc., Dalton Trans.*, 1983, 2599.
3 B. D. Dombek, *Organometallics*, 1985, **4**, 1707.
4 Y. Kiso and K. Saeki, *Bull. Chem. Soc. Jpn.*, 1987, **60**, 617.
5 J. F. Knifton, *J. Chem. Soc., Chem. Commun.*, 1983, 729.
6 J. Pursiainen, T. A. Pakkanen and J. Jaaskelainen, *J. Organomet. Chem.*, 1985, **290**, 85.
7 J. Pursiainen, T. A. Pakkanen and K. Smolander, *J. Chem. Soc., Dalton Trans.*, 1987, 781.
8 J. Pursiainen, T. A. Pakkanen, B. T. Heaton, C. Seregni and R. G. Goodfellow, *J. Chem. Soc., Dalton Trans.*, 1986, 681.
9 A. Fumagalli and G. Ciani, *J. Organomet. Chem.*, 1984, **272**, 91.
10 A. C. Street, Ph.D. Thesis, University of Southampton, 1987.
11 J. Evans, J.-X. Gao, H. Leach and A. C. Street, *J. Organomet. Chem.*, 1989, **372**, 61.
12 A. A. Arduini, A. A. Bahsoun, J. A. Osborn and C. Voelker, *Angew Chem., Int. Ed. Engl.*, 1980, **19**, 1024; A. A. Bahsoun, J. A. Osborn, C. Voelker, J. J. Bonnet and G. Lavigne, *Organometallics*, 1982, **1**, 1114; J. A. Clucas, M. M. Harding, B. S. Nicholls and A. K. Smith, *J. Chem. Soc., Chem. Commun.*, 1984, 319.
13 J. A. Hriljac, E. M. Holt and D. F. Shriver, *Inorg. Chem.*, 1987, **26**, 2943; V. E. Lopatin and S. P. Gubin, *Metallorganich. Khim*, 1989, **2**, 668 (*Organomet. Chem. USSR*, 1989, **2**, 345).
14 M. J. Mays, P. R. Raithby, P. L. Taylor and K. Henrick, *J. Chem. Soc., Dalton Trans.*, 1984, 959.
15 J. Evans, P. M. Stroud and M. Webster, *J. Chem. Soc., Chem. Commun.*, 1989, 1029.
16 R. R. Schrock and J. A. Osborn, *J. Am. Chem. Soc.*, 1971, **93**, 2397.
17 B. F. G. Johnson, J. Lewis, A. G. Orpen, P. R. Raithby and G. Süss, *J. Organomet. Chem.*, 1979, **173**, 187; M. R. Churchill, L. R. Beanan, H. J. Wasserman, C. Bueno, Z. A. Rahman and J. B. Keister, *Organometallics*, 1983, **2**, 1179.
18 J. B. Keister, M. W. Payne and M. J. Muscatella, *Organometallics*, 1983, **2**, 219.
19 L. Vallarino, *J. Chem. Soc.*, 1957, 2287.
20 G. M. Sheldrick, SHELXS 86, Program for Crystal Structure Determination, University of Göttingen, 1986.
21 G. M. Sheldrick, SHELX 76, Program for Crystal Structure Determination, University of Cambridge, 1976.
22 W. C. Hamilton, *Acta Crystallogr.*, 1965, **18**, 502; D. Rogers, *Acta Crystallogr., Sect. A*, 1981, **37**, 734.
23 *International Tables for X-Ray Crystallography*, Kynoch Press, Birmingham, 1974, vol. 4, pp. 99–101, 149–150.
24 C. K. Johnson, ORTEP II, Report ORNL-5158, Oak Ridge National Laboratory, 1976.
25 D. M. Dalton, D. J. Barnett, T. P. Duggan, J. B. Keister, P. T. Malik, S. P. Modi, M. R. Shaffer and S. A. Smesko, *Organometallics*, 1985, **4**, 1854.
26 J. Evans, P. M. Stroud and M. Webster, *Acta Crystallogr., Sect. C*, 1990, **46**, 2334.
27 J. Evans, B. F. G. Johnson, J. Lewis, T. W. Matheson and J. R. Norton, *J. Chem. Soc., Dalton Trans.*, 1978, 626.
28 A. M. Bradford, G. Douglas, L. Manojlović-Muir, K. W. Muir and R. J. Puddephatt, *Organometallics*, 1990, **9**, 409.
29 C. H. Wei, *Inorg. Chem.*, 1969, **8**, 2384.
30 B. T. Heaton, L. Longhetti, D. M. P. Mingos, C. E. Briant, P. C. Minshall, B. R. C. Theobald, L. Garlaschelli and U. Sartorelli, *J. Organomet. Chem.*, 1981, **213**, 333.

31 J. Pursiainen and T. A. Pakkanen, *J. Organomet. Chem.*, 1986, **315**, 353.

32 M. I. Bruce, M. L. Williams, J. M. Patrick, B. W. Skelton and A. H. White, *J. Chem. Soc., Dalton Trans.*, 1986, 2557.

33 J. Evans, P. M. Stroud and M. Webster, *J. Chem. Soc., Dalton Trans.*, 1991, 1017.

Received 21*st January* 1991; *Paper* 1/00277E